



# Pro-inflammatory responses to PM<sub>0.25</sub> from airport and urban traffic emissions

Rui-Wen He<sup>a,b</sup>, Farimah Shirmohammadi<sup>c</sup>, Miriam E. Gerlofs-Nijland<sup>a</sup>,  
Constantinos Sioutas<sup>c</sup>, Flemming R. Cassee<sup>a,b,\*</sup>

<sup>a</sup> National Institute for Public Health and the Environment (RIVM), P.O. Box, 2720 BA Bilthoven, the Netherlands

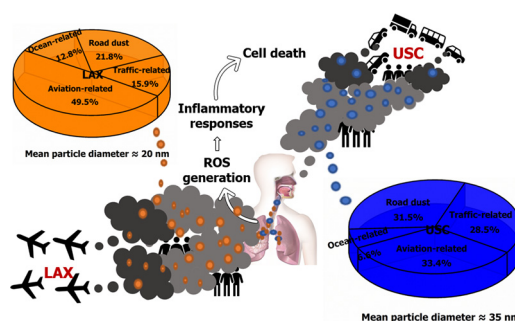
<sup>b</sup> Institute for Risk Assessment Sciences, Utrecht University, P.O. Box 80178, 3508 TD Utrecht, the Netherlands

<sup>c</sup> University of Southern California, Department of Civil and Environmental Engineering, 3620 S Vermont Ave, Los Angeles, CA 90089, USA

## HIGHLIGHTS

- Aviation emission was the main contributor to PM<sub>0.25</sub> from a major airport.
- Urban area PM<sub>0.25</sub> was dominated by road traffic (traffic emission and road dust).
- Airport-related PM<sub>0.25</sub> exerts similar toxicity compared to PM<sub>0.25</sub> from urban traffic.

## GRAPHICAL ABSTRACT



## ARTICLE INFO

### Article history:

Received 23 February 2018

Received in revised form 7 May 2018

Accepted 30 May 2018

Available online 5 June 2018

Editor: Lidia Morawska

### Keywords:

PM<sub>0.25</sub>

Aviation emission

Traffic emission

Oxidative potential

Pro-inflammation

## ABSTRACT

Air traffic is rapidly growing, raising concerns about the air pollution in the surroundings of airports and its impact on public health. However, little is known about the impact of air pollution sources on air quality and health in the vicinity of airports. In this study, the sources and adverse health effects of airport-related particulate matter (PM) were investigated and compared to those of urban traffic emissions. Ambient PM<sub>0.25</sub> were collected at the Los Angeles International Airport (LAX) and at a central Los Angeles site (USC campus), along with PM<sub>2.5</sub> collected directly from turbine and diesel engines. The particle chemical composition, oxidative potential (OP) (ascorbic acid (AA), and electron spin resonance (ESR) assay) as well as their reactive oxygen species (ROS) activity, inflammatory potential (interleukin (IL) 6 and 8 and tumor necrosis factor (TNF)-α) and cytotoxicity on human bronchial epithelial (16HBE) cells were assessed. Chemical composition measurements confirmed that aircraft emissions were the major source to LAX PM<sub>0.25</sub>, while the sources of the USC samples were more complex, including traffic emissions, suspended road and soil dust, and secondary aerosols. The traffic-related transition metals (Fe and Cu) in LAX and USC samples mainly affected OP values of particles, while multiple factors such as composition, size distribution and internalized amount of particles contributed to the promotion of ROS generation in 16HBE cells during 4 h exposure. Internalized particles in cells might also play an important role in activating inflammatory responses during cell recovery period, with LAX particles being more potent. Our results demonstrated considerable toxicity of airport-related particles, even at low exposure concentrations, suggesting that airport emission as source of PM<sub>0.25</sub> may also contribute to the adverse effects on public health attributable to PM. The potency of such particles is in the same range as those collected at a site in urban area impacted heavily by traffic emissions.

© 2018 Elsevier B.V. All rights reserved.

\* Corresponding author at: National Institute for Public Health and the Environment (RIVM), P.O. Box, 2720 BA Bilthoven, the Netherlands.  
E-mail address: [flemming.cassee@rivm.nl](mailto:flemming.cassee@rivm.nl) (F.R. Cassee).

## 1. Introduction

Due to the rapid development of the aviation industry and high demand for air transportation, the concomitant airport pollution has attracted increasing attention in recent years (Masiol and Harrison, 2014). Airport particulate matter (PM) emissions are the known source of air pollution in the proximity of an airport (Hu et al., 2009; Hudda et al., 2014). These particles, however, are not only from aircraft emissions (engine exhaust and non-exhaust emissions from aircraft), but also emissions from other sources like the ground traffic operations for transporting people and goods (Masiol and Harrison, 2014). However, current information regarding contributions of the relevant sources to airport PM emissions is inadequate, which hinders our ability to accurately assess the population risks associated with the exposure to these emissions.

Large airports are often located in the proximity of metropolises, consequently airport emissions may have considerable impact on public health in the surrounding urban areas. Barrett et al. (2010) estimated that around 8000 premature mortalities were attributable to aircraft cruise emissions globally every year (Barrett et al., 2010). Touri et al. (2013) examined the impact of airport pollution exposure on respiratory health by evaluation of studies on occupational exposure. Although the link between respiratory health effects and airport pollution exposure was shown in a few occupational studies, the correlation was weak and needs further research (Touri et al., 2013). Therefore, understanding the associated risks of exposure to airport-related PM in comparison with other major contributors to urban PM such as vehicle emissions are of great significance to public health officials and legislators.

PM is a rather complex mixture that could differ in size distribution and chemical composition depending on emission sources. Both size distribution and composition are major critical factors influencing particle toxicity (Kelly and Fussell, 2012). Particles in the nanometer-size range typically account for the majority of total particle number concentrations in airport areas (Masiol and Harrison, 2014). A recent LAX airport study shown that the mean diameter of particles from the LAX is around 20 nm that is distinctly smaller than particles emitted from the urban traffic area (USC samples: mean diameter  $\approx$  35 nm) (Shirmohammadi et al., 2017b). These nano-sized airport-related particles result in a higher surface area/mass ratio compared to micron-sized PM, which allows more organic and inorganic species to be adsorbed and/or absorbed on their surface. This, in turn, could increase the particle toxicity per unit inhaled mass (Li et al., 2003; Nel et al., 2006). Many relevant toxic effects of PM might be triggered through PM-induced oxidative stress due to reactive oxygen species (ROS) generation in cells (Ayres et al., 2008; Xiang et al., 2016). PM-induced ROS can oxidize lipids and damage DNA, thereby impairing natural defense mechanisms, and lead to excessive production of inflammatory mediators, which are highly related to many respiratory and lung inflammatory diseases. In particular, small particle size and PM species including elemental carbon (EC), a number of organics as well as soluble transition metals (including Ni, V, Fe, and Cu) can have significant effects on the toxicity of PM as evidenced by previous studies (Aust et al., 2002; Kelly and Fussell, 2012; Loxham et al., 2013). However, there is a general lack of information on the health hazards of aviation-released PM compared to that of other mobile transportation sources such as road traffic.

The primary goal of the study presented here was to explore the health hazards of two important PM sources in relation to their PM composition. We hypothesized that airport-related PM<sub>0.25</sub> can induce comparable cytotoxicity to particles collected from an urban area, impacted mostly by road traffic emissions. To test this hypothesis, we collected PM<sub>0.25</sub> samples downwind the Los Angeles International airport and in the downtown area of Los Angeles, CA, along with PM samples directly collected from the exhaust of a turbine and a diesel engine, then examined how these different PM samples affect the biological responses in human bronchial epithelial (16HBE) cells.

## 2. Materials and methods

### 2.1. PM sampling

#### 2.1.1. Urban air PM samples

Ambient PM<sub>0.25</sub> samples were collected in two locations in Los Angeles, as discussed in more detail by Shirmohammadi et al. (2017a). One sampling site was near the residential area of Playa del Rey, at a South Coast Air Quality Management District (AQMD) LAX Hastings monitoring site, which is located adjacent to the downwind Los Angeles International Airport (LAX). The PM<sub>0.25</sub> collected in this site was mainly influenced by the airport emissions and to a lesser extent by shore ocean breeze, and are less affected by traffic emissions (Shirmohammadi et al., 2017a). The other site was in central Los Angeles, at the University of Southern California (USC), roughly 150 m from- and immediately downwind the major freeway (I-110). Samples collected here mainly represent urban mixed particles, mostly dominated by road traffic emissions (Minguillón et al., 2008; Sowlat et al., 2016).

Personal Cascade Impactor Samplers (PCIS) (SKC, Inc., Eighty-Four, PA, USA) were used for sampling PM at the flow rate of 9 lpm (Misra et al., 2002). The sampling duration for each sample was 7 days from late October to early December of 2016 (for a total of 5 weeks). Each site was visited once a week to collect samples and load new filters. Flow rates were checked during the visit to ensure proper performance of the PCIS samplers. PM was classified in two particle collection size ranges: accumulation mode (0.25–2.5  $\mu$ m, PM<sub>2.5–0.25</sub>) and quasi-ultrafine mode (<0.25  $\mu$ m, PM<sub>0.25</sub>). Only PM<sub>0.25</sub> samples have been used for the work discussed in this paper, as they were considered more representative of direct primary emissions compared to the accumulation mode range that contains a higher fraction of regional aerosols (Shirmohammadi et al., 2017a). During the sampling period, one PCIS loaded with 37-mm quartz filters (Whatman International Ltd., Maidstone, England) was used for organic chemical speciation measurements (details can be found in Shirmohammadi et al., 2017a). The other three PCISs were loaded with 37-mm Teflon filters (Pall Life Sciences, 3- $\mu$ m pore, Ann Arbor, MI) for gravimetric measurements to determine mass concentration as well as for the additional chemical and biological analyses discussed in this study.

#### 2.1.2. Turbine and diesel samples

Turbine and diesel samples were collected directly from diluted exhaust of a Fighting Falcon turbine engine (F100, Pratt & Whitney, East Hartford, Connecticut, USA) and a low-sulfur fuel diesel (EN 590) engine (Bredenoord, 35 KVA Silent, Apeldoorn, Netherlands), respectively, by means of a versatile aerosol concentration enrichment system (VACES) (Kim et al., 2001) as well as a high-volume cascade impactor (HVCI) sampler (Demokritou et al., 2002) in this study. Minor flows of the VACES were used to collect droplets containing particles into a BioSampler (SKC, Inc., Eighty-Four, PA, USA) as well as passing the concentrated aerosol through a diffusion dryer and subsequently collect PM on 47-mm Teflon filters (Pall Life Sciences, 2- $\mu$ m pore, Ann Arbor, MI, USA) for the biological and chemical analyses, respectively. Albeit that the VACES was equipped with a PM<sub>2.5</sub> size selective inlet, the vast majority of the particles from both test engines were <0.1  $\mu$ m. Sampling time for each day lasted for 8 h and a filter was collected in parallel to the BioSampler, then a new filter was loaded for the next sampling day, resulting in 1 turbine sample and 3 diesel samples were collected. Flow rates, heating and cooling temperatures, and particle number concentration as well as concentration enrichment of the VACES were checked every 2 h to ensure proper performance. The HVCI consists of different impaction stages to collect particles in different size ranges. 3 impaction stages (cut-points at 10, 2.5 and 0.1  $\mu$ m, respectively) were selected in this study, and downstream of the third stage, a backup TE 38 filter (Whatman, 5- $\mu$ m pore, Dassel, Niedersachsen, Germany) was placed for collecting the ultrafine particles (<0.1  $\mu$ m) for chemical

analysis. All filters were weighed before and after sampling to determine particle mass loadings and then stored in petri dishes at 4 °C in the dark.

## 2.2. Filters extraction

Teflon filters (5 LAX and 5 USC filters from PCIS, 1 turbine and 3 diesel filters from VACES) were immersed by 2 mL methanol (HPLC grade) in a petri dish, followed by sonication (Sonorex RK-52, 60/120 kW, 35 kHz, Bandelin, Berlin, Germany) for 1 min. The filters were then flipped over with clean tweezers and were sonicated again for 1 min, a process that was repeated for three consecutive times. The extract was transferred into a vial, then 5 LAX extracts, 5 USC extracts and 1 turbine extract were dried respectively overnight at 30 °C in an incubator. For diesel samples, 3 diesel extracts were combined before drying. All the filters were also weighed after the extraction process to determine the extraction efficiency, which was around 90% in this study. Dried extracts (5 LAX, 5 USC, 1 turbine and 1 diesel samples) were re-suspended in 1 mL Hanks' Balanced Salt solution (HBSS, Thermo Fisher Scientific Inc., the Netherlands), which can maintain cells osmotic balance during in vitro assay.

## 2.3. Chemical analysis

Filter samples (details in Section 2.1) collected at LAX and USC as well as from the exhaust of the turbine and diesel engines (from HVCI) were analyzed to quantify the chemical PM constituents. The analytical procedures were described in more detail by Shirmohammadi et al. (2017a). Briefly, both EC and OC content of all weekly samples were quantified using 1 cm<sup>2</sup> punch of each quartz filters. The United States National Institute for Occupational Safety and Health Thermal Optical Transmission method was applied in EC and OC analysis (Birch and Cary, 1996). To measure the total elemental composition of the PM, a section of each Teflon filter was digested in a mixture of 1.5 mL of 16 M nitric acid, 0.5 mL of 12 M hydrochloric acid and 0.2 mL of hydrofluoric acid using a microwave-aided solubilization protocol (Shirmohammadi et al., 2017a). The digests were then analyzed using a high resolution (magnetic sector) inductively coupled plasma mass spectrometer (SF-ICPMS, Thermo-Finnigan Element 2).

## 2.4. Oxidative potential assays

### 2.4.1. Ascorbic acid (AA) depletion assay

The AA assay measures the rate of AA consumption by a known amount of PM and was used to measure the redox activity of the ambient and engine exhaust PM samples of this study. 200 µg/mL PM re-suspensions (in HBSS) were diluted in ultrapure water (1:15) to a concentration of 12.5 µg/mL. Briefly, 160 µL of 12.5 µg/mL PM suspension was added to a 96-well flat-bottomed UV plates (VWR, Breda, Netherlands). All samples were incubated in a spectrophotometer (spectraMAX 190; Molecular Devices, Sunnyvale, USA) for 10 min at 37 °C. 20 µL of 2 mM AA was then added and measured by a microplate reader at 265 nm every 2 min for 2 h. For AA depletion assay experiment, 160 µL of domestic oil burning furnace particles (DOFA, US EPA, RTP, NC) suspension at 12.5 µg/mL and HBSS diluted in dH<sub>2</sub>O (1:15) were used as the positive, and negative controls, respectively. The results were expressed as nmol/s of AA depletion per µg PM.

### 2.4.2. Electron spin resonance (ESR) assay

ESR assay is selected to detect the PM-induced hydroxyl radical (OH•) generation, which is mainly generated via Fenton-type reaction. Spin trap 5,5-dimethyl-1-pyrroline-*N*-oxide (DMPO) was applied in presence of hydrogen peroxide. In brief, 25 µL of 200 µg/mL PM re-suspension (in HBSS) was mixed with 50 µL of 0.05 M DMPO (kept in the dark) and 25 µL 0.5 M hydrogen peroxide (H<sub>2</sub>O<sub>2</sub>) in a vortex mixer for 5 s and then placed in shaking water bath at 37 °C for

15 min' incubation. The suspension was then placed in the vortex mixer again for 15 s followed by a transfer into a 50 µL glass capillary to measure. A MS-300 ESR spectrometer (Magnetech, Berlin, Germany) was utilized to measure the DMPO-OH quartet signal. The following ESR settings at room temperature were used for all measurements: magnetic field: 337 mT, range: 7 mT, sweep time: 30 s, number of scans: 3, modulation amplitude: 0.2 mT, receiver gain: 2E2. For ESR assay, DOFA suspension at 1000 µg/mL and HBSS were used as the positive, and negative control, respectively. The results were expressed as the total amplitudes of DMPO-OH quartet in arbitrary units (A.U.) per µg PM.

## 2.5. Cell culture

Human bronchial epithelial (16HBE) cells used in Braakhuis et al. (2016) were cultured in Dulbecco Modified Eagle Medium (DMEM)/F-12 medium, L-Glutamine (1%), fungizone (1%), fetal bovine serum (5%), and 1% weight per volume penicillin/streptomycin in an incubator with 5% CO<sub>2</sub> at 37 °C. All culture media and supplements were purchased from Life Technologies (Thermo Fisher Scientific Inc., the Netherlands).

## 2.6. Cell viability

The 3-(4,5-dimethylthiazol-2-yl)-5-(3-carboxymethoxyphenyl)-2-(4-sulfophenyl)-2H-tetrazolium (MTS) assay, a colorimetric method for determining the number of viable cells, was used to study cytotoxicity due to exposure to PM according to the manufacturer procedure (Promega, Fitchburg, Wisconsin, USA). Briefly, 16HBE cells were seeded into 96-well plates with  $2 \times 10^5$  cells/mL and cultured for 24 h to reach ~80% confluence. Subsequently, the medium was replaced by the 100 µL non-serum fresh culture medium to prevent a protein corona around the particles. Two samples with relatively high mass filter loadings (L4: LAX week 4 and U4: USC week 4) were firstly chosen to establish the range for a concentration-response relationship (5 to 160 µg/mL). Cells were exposed to PM for 4 h after which the culture media was refreshed with serum-free fresh culture medium without PM for a 20 h recovery period. The culture media from recovery period were collected and stored at -20 °C for testing cytokine release. Next, cells were washed with HBSS and incubated with serum-free fresh culture medium containing MTS reagent (medium: MTS reagent = 10:1) for 1 h following absorbance measurement by a microplate reader at 490 nm (SpectraMax M2; Molecular Devices, Sunnyvale CA, USA). Fresh HBSS (containing no PM) was used as negative control. Based on the concentration-response curve, the concentration points corresponding to 80% of viability were set as the exposure concentration for the repetition of MTS assay for all PM samples (Fig. S2).

## 2.7. Reactive oxygen species (ROS) activity

Changes in intracellular ROS level after PM exposure were detected using the fluorescent dye 2', 7'-dichlorodihydrofluorescein diacetate (H<sub>2</sub>-DCFDA) (Thermo Fisher Scientific Inc., Eindhoven, the Netherlands) methodology, which is based on the oxidation of nonfluorescent H<sub>2</sub>-DCFDA by intracellular ROS to highly fluorescent 2',7'-dichlorofluorescein (DCF). H<sub>2</sub>-DCFDA in the assay is used as an indicator for intracellular generated reactive oxygen species (ROS). Similarly to the seeding process followed for cell viability testing, cells were washed with HBSS before adding 100 µL H<sub>2</sub>-DCFDA (10 µM, dilute in HBSS) probe (in the dark). After 45 min incubation, the probe was removed, and cells were washed again, and the plate was measured with 100 µL HBSS using microplate reader (SpectraMax M2; Molecular Devices, Sunnyvale CA, USA) to determine the basal ROS production over the time. The cells were then exposed to all PM samples with serum-free fresh colorless culture medium and the plate was measured after 1 h, 2 h,



4 h exposure and 20 h recovery. 0.5% H<sub>2</sub>O<sub>2</sub> and fresh HBSS (no PM) were used as positive and negative controls, respectively.

## 2.8. Release of inflammatory mediators

To test the effects of particles on pro-inflammatory mediators expression, the release of IL-6, IL-8 and tumor necrosis factor  $\alpha$  (TNF- $\alpha$ ) proteins from 16HBE cells was determined for LAX and USC samples with the supernatants collected from MTS assay using Luminex Multiplex Kit (Millipore, Merck, Darmstadt, Germany). For turbine and diesel samples, only IL-8 release was determined using the Enzyme-linked Immunosorbent Assay (ELISA) Kit (eBioscience, San Diego, USA). Fresh HBSS (no PM) was used as the negative control.

## 2.9. Statistical analysis

Correlations between elemental composition and oxidative potential (OP) were analyzed using Spearman rank correlation coefficient. Statistical comparison test was conducted using one-way ANOVA, significant differences were defined as  $p < 0.05$ .

## 3. Results

### 3.1. Characteristics of particles

The measured elements were assigned to four categories, each representing a specific emission source; these categories were aviation, ocean spray, road dust, and traffic. S, as the most abundant element in aircraft emissions, was considered as the aviation-related species (Kinsey et al., 2011). As the LAX site is located near the Pacific Ocean, particle-bound Na was considered as the ocean-related element in the form of sea salt. Al, Ca, Ti and K reported as the trace elements for suspended road dust (Marcazzan et al., 2001) were considered as road dust elements for LAX and USC particles (Al, Ca, and Ti were considered as road dust elements for turbine and diesel particles without K). While Mn, Fe, Cu, Zn, Ba, Pb, Ni, and Mg were elements associated with the traffic emissions, including combustion of fuel and lubricating oil as well as abrasion of brake, engine and tire wear (Maier et al., 2010; Pant and Harrison, 2013). For the LAX samples, aviation-related element (S) accounted for the largest fraction at 49.5%, followed by road dust elements (Al, Ca, Ti and K) and traffic-related elements (Mn, Fe, Cu, Zn, Ba, Pb, Ni and Mg) at 21.8% and 15.9%, respectively. In contrast, the emissions from traffic (28.5%), road dust (31.5%) and aviation (33.4%) were represented equally in the USC samples. In addition, ocean-related element had a higher contribution to the total elemental fraction for the LAX samples (12.8%) than in USC samples (6.60%) (Fig. 1a), which can be explained by the proximity of the LAX to the Pacific Ocean, as noted earlier.

As presented in Fig. 1b, aviation element contributed to the largest fraction in turbine sample at 82.9%, which corroborated the use of this element (S) as a tracer of aviation-related emissions in the smaller PM size range. Road dust (Al, Ca, and Ti), traffic and ocean markers accounted for much smaller fractions of 9.53%, 6.54%, and 1.04%, respectively. For diesel samples, traffic-related elements were the major contributors (54.1%) to the total elemental fraction, followed by ocean marker at 23.2%. The remainder was divided by aviation and road dust markers, with similar fractions of 12.2% and 10.4%, respectively. The mass fractions of the PM<sub>0.25</sub> measured species, including trace elements and metals as well as organic carbon (OC) and elemental carbon (EC) can be found in Table S1. The ambient concentrations of these species are reported in detail in Shirmohammadi et al. (2017a). EC and OC were omitted from our statistical analyses because their mass fractions in the USC and LAX samples were virtually identical (as seen in Table S1) and their inclusion to the statistical analysis did not provide any meaningful insight or conclusions.

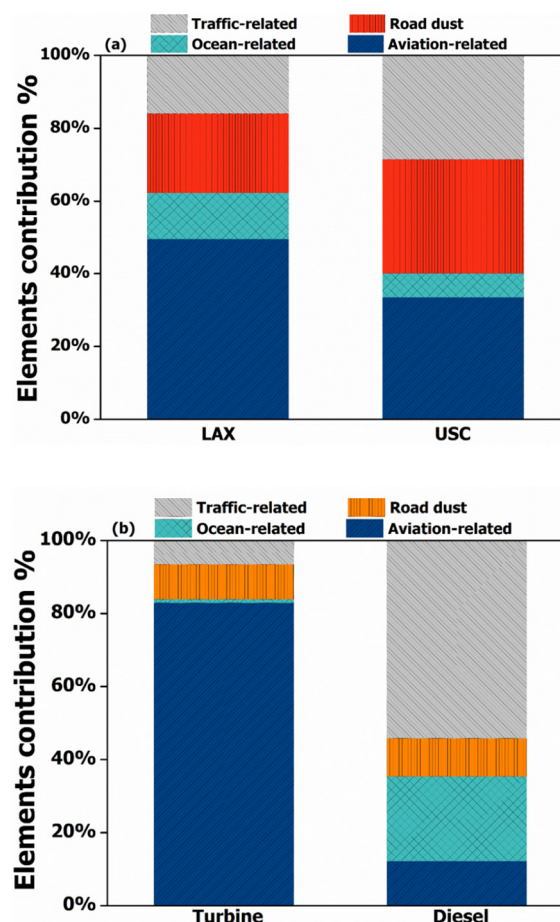


**Fig. 1.** Elemental contributions in PM from LAX and USC (a) as well as turbine and diesel engines (b). S was considered as aviation-related element, Na as ocean-related element, and Mn, Fe, Cu, Zn, Ba, Pb, Ni and Mg as traffic-related elements in both (a) and (b). Al, Ca, Ti and K were considered as road dust elements in a (red), while Al, Ca, and Ti as road dust elements in b (orange).

### 3.2. Oxidative potential assays (AA and ESR)

The oxidative potentials (OP) measured by AA and ESR of PM<sub>0.25</sub> sampled at LAX and USC are illustrated in Fig. S1, using the ratios of PM samples divided by negative control (NC) values of each assay. A significant positive correlation was observed between OP<sub>AA</sub> and OP<sub>ESR</sub> ( $R = 0.81$ ,  $p < 0.05$ ,  $n = 10$ , Table S2).

To evaluate and compare the OP level of different PM samples, the geometric mean (GM) values of OP<sub>AA</sub> and OP<sub>ESR</sub> are presented in Table 1 for all PM samples. For both LAX and USC samples, OP<sub>AA</sub> and OP<sub>ESR</sub> values were significantly higher than the value of negative control ( $p < 0.05$ ), with LAX samples showing relatively lower values compared to USC samples ( $0.33 \pm 0.10$  vs  $1.14 \pm 0.18$  for AA,  $1.97 \pm 0.51$  vs  $3.58 \pm 0.24$  for ESR). OP<sub>AA</sub> and OP<sub>ESR</sub> levels in turbine samples were higher than the levels of diesel samples ( $1.11 \pm 0.04$  vs  $0.53 \pm 0.06$  for AA,  $0.83 \pm 0.07$  vs  $0.59 \pm 0.11$  for ESR). Both PM samples showed significant OP except the diesel PM OP<sub>ESR</sub> value, which was comparable to OP value of the NC.

### 3.3. Cell viability

Cell viability, an important indicator of toxicity, was measured after 24 h, including 4 h particle exposure and 20 h recovery period. One low (10  $\mu\text{g/mL}$ ) and one high (100  $\mu\text{g/mL}$ ) exposure level were used for all samples, as shown in Fig. 2. Overall, 16HBE cells treated at 10 and 100

**Table 1**

Geometric mean of oxidative potential (AA and ESR) values of LAX, USC, turbine, and diesel samples as well as negative and positive controls.

	AA (nmol AA/s/μg)	ESR (A.U./1000/μg)
LAX (n = 5)	0.33 ± 0.10	1.97 ± 0.51
USC (n = 5)	1.14 ± 0.18	3.58 ± 0.24
Turbine	1.11 ± 0.04	0.83 ± 0.07
Diesel	0.53 ± 0.06	0.59 ± 0.11
Negative control (dH <sub>2</sub> O)	0.08 ± 0.02	0.49 ± 0.02
Positive control (DOFA)	1.36 ± 0.13	11.4 ± 0.37

μg/mL particles showed little cytotoxic effects, with the exceptions of U1 (81.8%) and U2 (79.6%) at 100 μg/mL, for which cell viabilities were around 80%, implying more cell deaths. To further study cellular responses after exposure, the lower exposure dose (10 μg/mL) was used in subsequent study tests.

### 3.4. Reactive oxygen species (ROS) activity

Intracellular ROS generation was measured after 1, 2, and 4 h exposure and 20 h recovery for all the samples to examine the oxidative potential of the particles by an additional method. The level of ROS was illustrated using ratios between samples and negative control (Fig. 3 and Fig. S3). After exposure to 10 μg/mL particles, the ROS levels in 16HBE cells were significantly elevated ( $p < 0.05$ ), and a slowly increasing trend was observed from 1 h to 4 h in all samples. On average, USC samples caused a slightly higher ROS generation than LAX samples per unit mass, while turbine samples showed a greater effect on ROS induction than diesel samples ( $p < 0.05$ ). After 20 h recovery, ROS production decreased to comparable level to the negative control for LAX, and USC samples.

### 3.5. Correlation between oxidative potential indicators and PM composition

We selected  $OP_{AA}$ ,  $OP_{ESR}$  and  $OP_{ROS}$  at 1, 2, and 4 h to calculate the Spearman's correlation coefficient with chemical species in LAX and USC samples (Table 2). It was shown that  $OP_{AA}$ ,  $OP_{ESR}$  and  $OP_{ROS}$  at 1, 2, and 4 h significantly correlated with traffic-related transition metals (Fe and Cu, Spearman R: 0.65–0.87;  $p < 0.05$ ). Some trace elements that are ingredients of road and soil dust (e.g. Ti, Pb and Ca) also showed positive correlation with  $OP_{AA}$  and  $OP_{ESR}$  (Spearman R: 0.65–0.77;  $p < 0.05$ ) but not with the  $OP_{ROS}$ .

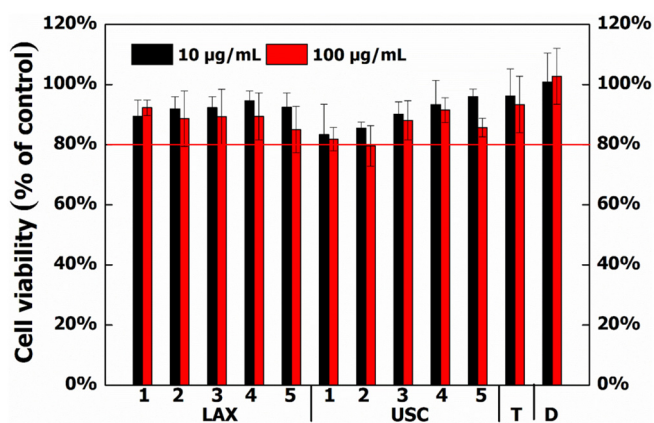


**Fig. 2.** 16HBE cell viability tested by MTS assay for all PM samples at 10 and 100 μg/mL. T and D denote turbine and diesel samples, respectively. 1, 2, 3, 4, and 5 refer to the sampling week at LAX and USC.

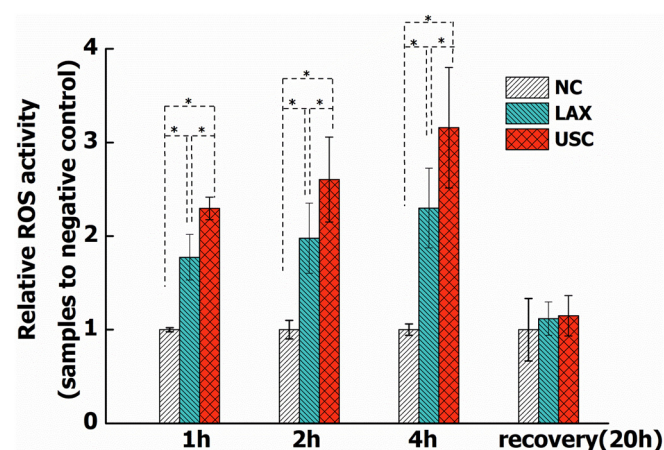


**Fig. 3.** Average relative ROS activity in 16HBE cells after 1, 2, 4 h exposure and 20 h recovery to  $PM_{0.25}$  from LAX, and USC (compared to the negative control, NC), \* represents significant difference at  $p < 0.05$ .

### 3.6. Inflammatory mediators

The induction and release of inflammatory mediators (IL-6, IL-8 and TNF- $\alpha$ ) was observed in 16HBE cells, and is expressed as ratios between samples and negative control (Fig. 4). The LAX samples induced higher release of the inflammatory mediators in 16HBE cells at 1.7, 1.8, and 1.4-fold increase for IL-6, IL-8 and TNF- $\alpha$ , respectively, while the release of IL-6, IL-8 and TNF- $\alpha$  induced by USC samples were at 1.3, 1.3, and 1.1-fold increase, respectively. However, no significant changes of IL-8 release were seen for turbine and diesel samples at 10 μg/mL.

## 4. Discussion

Our results demonstrate the adverse responses in human bronchial cells (16HBE), including effects on cell viability/cytotoxicity, ROS activity and inflammatory mediators release, after exposure to ambient  $PM_{0.25}$  collected near airport and urban sites as well as PM directly sampled from diluted exhaust of turbine and diesel engines. Elemental composition and oxidative potential of the PM samples seem to explain these biological responses.

Combustion of different fuels and the use of diverse engine types result in the emission of PM with distinctly different elemental composition. In line with several previous studies, S was found to be the most dominant element (82.9%) for turbine engine particles in this study due to the abundant S content in aviation fuel (Agrawal et al., 2008; Kinsey et al., 2011). In comparison, diesel exhaust particles were dominated (54.1%) by elemental markers of fuel and lubricant oil combustion, such as Mn, Fe, Cu, Zn, Ba, Ni, Pb, and Mg (Lin et al., 2005; Wang et al., 2003). An appreciable (although lower than that of turbine engines) S fraction (12.2%) was measured in diesel samples, probably due to the S content in diesel oil and fuel (Shields et al., 2007).

**Table 2**

Spearman's correlation coefficients (R) between the OP measures (AA, ESR and ROS) and chemical species for LAX and USC samples.

Species	AA	ESR	ROS <sub>1h</sub>	ROS <sub>2h</sub>	ROS <sub>4h</sub>
Cu	0.87*	0.80*	0.81*	0.78*	0.71*
Fe	0.85*	0.76*	0.77*	0.73*	0.65*
Ca	0.77*	0.72*	0.64	0.60	0.50
Ti	0.71*	0.65*	0.59	0.53	0.41
Pb	0.70*	0.46	0.60	0.65*	0.67*
Sum of traffic-related elements	0.78*	0.71*	0.67*	0.64	0.55

\*  $p < 0.05$ .



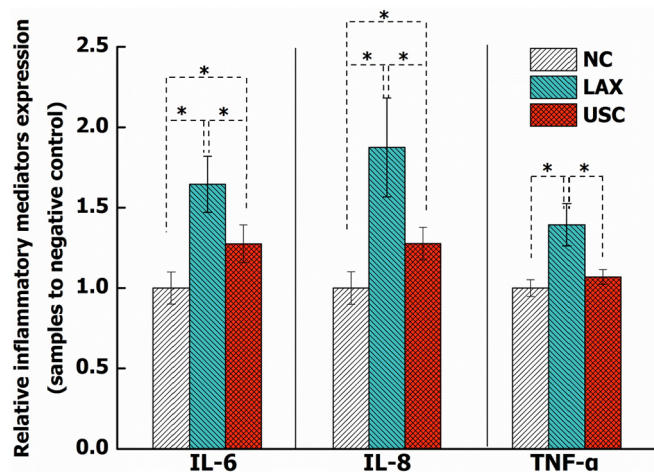


Fig. 4. Relative expression of inflammatory mediators (IL-6, IL-8, and TNF- $\alpha$ ) after 20 h recovery on 16HBE cells for LAX and USC samples (compared to the negative control, NC). \* represents significant difference at  $p < 0.05$ .

The elemental composition of PM<sub>0.25</sub> from LAX showed some differences compared to aircraft turbine engine samples. S (49.5%) was still the most abundant element for LAX samples, while the contributions of road dust (21.8%), vehicle emissions (15.9%), and ocean related elements (12.9%) were higher than those of the engine samples. This was a result of the influence of not only aircraft emissions, but also ground support transportation at the airport as well as the seaside location of LAX on the composition of these urban samples (Masiol and Harrison, 2014; Shirmohammadi et al., 2017a). This suggests that, besides aviation activities, the contributions from surrounding traffic emissions and re-suspended road-dust to the airport-related particles are not negligible. In contrast, the elemental contributions in USC sample differed considerably compared to diesel engine sample. Traffic, road dust related elements as well as S accounted for similar large fractions of the PM mass underscoring the contributions of emission sources such as suspended road dust and atmospheric secondary sulfate to urban particles besides exhaust emissions (Marcazzan et al., 2001; Pant and Harrison, 2013).

The oxidative potential (OP) assays, AA and ESR, used in this study mainly represent the level of metal mediated reactive oxygen species (ROS) in particles such as OH• by Fenton reaction. The values of OP<sub>ESR</sub> and OP<sub>AA</sub> both showed significant positive correlations with some dominant traffic-related metals such as Fe and Cu (Spearman  $R > 0.75$ ,  $p < 0.05$ , Table 2). Janssen et al. (2014) reported similar high correlations between OP<sub>ESR</sub> and OP<sub>AA</sub> (Spearman  $R > 0.85$ ), as well as the correlations with such transition metals (Janssen et al., 2014). This indicates that the level of transition metals in PM have a major impact on the induction of ROS. This in turn, might explain the higher OP<sub>ESR</sub> and OP<sub>AA</sub> levels for PM from USC and turbine engine as they contain more abundant traffic-related elements compared to LAX and diesel PM samples (Table 1).

In contrast, ROS regulation in cells relates to more components. When particles deposit on surface of cells after exposure, a number of particle-cell physicochemical interactions could take place, including catalysis of surface compositions, particle wrapping, intracellular uptake and biocatalysts (Nel et al., 2009; Øvrevik et al., 2015). Certain particle characteristics such as chemical composition, size distribution and surface area contribute actively to these interactions, often leading to oxidative stress due to access ROS generation (Øvrevik et al., 2015). It has been reported that transition metals play an important role in ROS generation; PM with higher level of transition metals such as Fe and Cu are capable of amplifying intracellular ROS generation (Aust et al., 2002; Schwarze et al., 2006), while the large surface area of ultrafine PM can provide more opportunities for catalyzing redox reactions (Nel et al.,

2006). Similar findings were shown in our study, in that, the USC as well as turbine particle samples that were more abundant in transition metals induced greater intracellular ROS generation during the exposure period compared to LAX and diesel samples, respectively ( $p < 0.05$ , Fig. 3 and Fig. S3).

To determine the influence of transition metals on ROS generation during the whole exposure period, the correlations between levels of OP<sub>ROS</sub> at 1, 2, and 4 h and the dominant transition metals (Fe and Cu) in PM<sub>0.25</sub> were calculated (Table 2). The significant and positive correlations between OP<sub>ROS</sub> at 1, 2, and 4 h and such metals at the first 1 h exposure (OP<sub>ROS</sub> at 1 h: Spearman  $R = 0.77$  to  $0.81$ ) confirmed the importance of these transition metals in ROS production. At the beginning of exposure, the release of redox active transition metals from particles might activate redox cycling (e.g. Fenton reaction) and promote a great intracellular ROS generation (Øvrevik et al., 2015). This similar ROS-formation principle may also explain the higher correlation coefficients between OP<sub>ROS</sub> at 1 h and OP<sub>AA</sub> and OP<sub>ESR</sub> ( $R = 0.95$  and  $0.84$ , Table S2). However, with cellular internalization of particles taking place, the size, surface area and internalized amount of particles might gradually dominate in intracellular ROS generation (Hussain et al., 2009; Li et al., 2008). Several studies reported that particles with smaller size have a higher likelihood entering into cells (Braakhuis et al., 2015; Gratton et al., 2008); their interaction with cellular membrane, subcellular organelles and biological systems can catalyze greater ROS production (Hussain et al., 2009; Li et al., 2008; Øvrevik et al., 2015). While the transition metals showed less influence on ROS generation during the cellular internalization period, this might explain the decrease in the correlation coefficients between OP<sub>ROS</sub> and these traffic-related metals over the course of the exposure (OP<sub>ROS</sub> at 2 h: Spearman  $R = 0.73$  to  $0.78$ , 4 h:  $R = 0.65$  to  $0.67$ , Table 2).

Furthermore, it has been reported that oxidative stress can activate transcription factors such as NF- $\kappa$ B and AP-1 (Reuter et al., 2010; Rincon and Irvin, 2012). This can lead to the transcription of pro-inflammatory mediators such as IL-6, IL-8 and TNF- $\alpha$ , the expression of which is directly related with asthma and some inflammatory pulmonary diseases. However, results from our study showed that inflammatory responses (IL-6, IL-8 and TNF- $\alpha$ ) could also be elicited after 20 h recovery even when ROS generation induced by PM was balanced to the control level. Although PM suspensions used for cell exposure were changed to particle-free culture media followed by a 20 h recovery period, several in vitro studies showed that small PM can cross the cell membrane and remain in cells (Gratton et al., 2008; Braakhuis et al., 2015), which may play an important role in inflammatory mediators' induction during the recovery period (Hussain et al., 2009). The smaller size distribution of LAX samples (Shirmohammadi et al., 2017a) might lead to greater internalized amount of particles, thus promoting the release of IL-6, IL-8 and TNF- $\alpha$  in 16HBE cells (Fig. 4).

The enhancement of ROS may disrupt the cellular oxidant-antioxidant balance, leading to inflammation and cytotoxicity. Excessive inflammation can result in the programmed cell death (Elmore, 2007). In this study, MTS values were all above 80%, indicating that cells showed low mortality after particles exposure (10  $\mu$ g/mL) in spite of at high level of oxidative stress. On the other hand, the results are also in accordance with the growing awareness that significant toxicity in cells such as enhanced ROS production and inflammatory responses can be induced even at high cell viability level (Valberg, 2004).

## 5. Summary and conclusions

In this study, we found that the aviation emissions were the major contributor to the total mass of PM<sub>0.25</sub> collected downwind a major airport. In contrast, PM collected in a busy urban area have more complex chemistry due to the contribution of multiple sources, including traffic emissions, suspended road dust and atmospheric secondary sulfates, which accounted for similar contributions. Moreover, elemental carbon and organic carbon content was very similar for these two locations. In

addition, our results demonstrated that airport-related PM<sub>0.25</sub>, even at relatively low exposure concentrations, possess toxic properties similar to the PM<sub>0.25</sub> emissions from urban traffic, suggesting that airport activity as a pollution source of PM<sub>0.25</sub> may also contribute to adverse effects on public health.

## Disclaimer

The content of this paper does not necessarily reflect the views and policies of the RIVM or those of the Netherlands Ministry of Infrastructures and Water Management. The authors have no conflict of interest to disclose.

## Acknowledgements

We thank Eric Gremmer, Daan L.A.C. Leseman, A. John F. Boere, Paul H. B. Fokkens from the National Institute for Public Health and the Environment (RIVM), Bilthoven, The Netherlands, and Yi-Xuan Li from the Institute for Risk Assessment Sciences, Utrecht University, Utrecht, The Netherlands, for their valuable assistance with the PM sampling and in vitro experiments. The support provided by China Scholarship Council (CSC) during the PhD period of Rui-Wen He in Utrecht University-Institute for Risk Assessment Studies is also acknowledged.

## Appendix A. Supplementary data

Supplementary data to this article can be found online at <https://doi.org/10.1016/j.scitotenv.2018.05.382>.

## References

- Agrawal, H., Sawant, A.A., Jansen, K., Miller, J.W., Cocker, D.R., 2008. Characterization of chemical and particulate emissions from aircraft engines. *Atmos. Environ.* 42, 4380–4392.
- Aust, A.E., Ball, J.C., Hu, A.A., Lighty, J., Smith, K.R., Straccia, A.M., Veranth, J.M., Young, W.C., 2002. Particle characteristics responsible for effects on human lung epithelial cells. *Res. Rep. (Health Eff. Inst.)* 1–65 (discussion 67–76).
- Ayres, J.G., Borm, P., Cassee, F.R., Castranova, V., Donaldson, K., Ghio, A., Harrison, R.M., Hider, R., Kelly, F., Kooter, I.M., Marano, F., Maynard, R.L., Mudway, I., Nel, A., Sioutas, C., Smith, S., Baeza-Squiban, A., Cho, A., Duggan, S., Froines, J., 2008. Evaluating the toxicity of airborne particulate matter and nanoparticles by measuring oxidative stress potential—a workshop report and consensus statement. *Inhal. Toxicol.* 20, 75–99.
- Barrett, S.R., Britter, R.E., Waitz, I.A., 2010. Global mortality attributable to aircraft cruise emissions. *Environ. Sci. Technol.* 44, 7736–7742.
- Birch, M., Cary, R., 1996. Elemental carbon-based method for monitoring occupational exposures to particulate diesel exhaust. *Aerosol Sci. Technol.* 25, 221–241.
- Braakhuis, H.M., Kloet, S.K., Kezic, S., Kuper, F., Park, M.V., Bellmann, S., van der Zande, M., Le Gac, S., Krystek, P., Peters, R.J., 2015. Progress and future of in vitro models to study translocation of nanoparticles. *Arch. Toxicol.* 89, 1469–1495.
- Braakhuis, H.M., Giannakou, C., Peijnenburg, W.J., Vermeulen, J., van Loveren, H., Park, M.V., 2016. Simple in vitro models can predict pulmonary toxicity of silver nanoparticles. *Nanotoxicology* 10, 770–779.
- Demokritou, P., Kavouras, I.G., Ferguson, S.T., Kouttrakis, P., 2002. Development of a high volume cascade impactor for toxicological and chemical characterization studies. *Aerosol Sci. Technol.* 36, 925–933.
- Elmore, S., 2007. Apoptosis: a review of programmed cell death. *Toxicol. Pathol.* 35, 495–516.
- Gratton, S.E., Ropp, P.A., Pohlhaus, P.D., Luft, J.C., Madden, V.J., Napier, M.E., DeSimone, J.M., 2008. The effect of particle design on cellular internalization pathways. *P. Natl. Acad. Sci.* 105, 11613–11618.
- Hu, S., Fruin, S., Kozawa, K., Mara, S., Winer, A.M., Paulson, S.E., 2009. Aircraft emission impacts in a neighborhood adjacent to a general aviation airport in Southern California. *Environ. Sci. Technol.* 43, 8039–8045.
- Hudda, N., Gould, T., Hartin, K., Larson, T.V., Fruin, S.A., 2014. Emissions from an international airport increase particle number concentrations 4-fold at 10 km downwind. *Environ. Sci. Technol.* 48, 6628–6635.
- Hussain, S., Boland, S., Baeza-Squiban, A., Hamel, R., Thomassen, L.C., Martens, J.A., Billon-Galland, M.A., Fleury-Feith, J., Moisan, F., Paire, J.-C., 2009. Oxidative stress and pro-inflammatory effects of carbon black and titanium dioxide nanoparticles: role of particle surface area and internalized amount. *Toxicology* 260, 142–149.
- Janssen, N.A., Yang, A., Strak, M., Steenhof, M., Hellack, B., Gerlofs-Nijland, M.E., Kuhlbusch, T., Kelly, F., Harrison, R., Brunekreef, B., 2014. Oxidative potential of particulate matter collected at sites with different source characteristics. *Sci. Total Environ.* 472, 572–581.
- Kelly, F.J., Fussell, J.C., 2012. Size, source and chemical composition as determinants of toxicity attributable to ambient particulate matter. *Atmos. Environ.* 60, 504–526.
- Kim, S., Jaques, P.A., Chang, M., Froines, J.R., Sioutas, C., 2001. Versatile aerosol concentration enrichment system (VACES) for simultaneous in vivo and in vitro evaluation of toxic effects of ultrafine, fine and coarse ambient particles part I: development and laboratory characterization. *J. Aerosol Sci.* 32, 1281–1297.
- Kinsey, J., Hays, M., Dong, Y., Williams, D., Logan, R., 2011. Chemical characterization of the fine particle emissions from commercial aircraft engines during the aircraft particle emissions experiment (APEX) 1 to 3. *Environ. Sci. Technol.* 45, 3415–3421.
- Li, N., Sioutas, C., Cho, A., Schmitz, D., Misra, C., Sempf, J., Wang, M., Oberley, T., Froines, J., Nel, A., 2003. Ultrafine particulate pollutants induce oxidative stress and mitochondrial damage. *Environ. Health Persp.* 111, 455.
- Li, N., Xia, T., Nel, A.E., 2008. The role of oxidative stress in ambient particulate matter-induced lung diseases and its implications in the toxicity of engineered nanoparticles. *Free Radic. Bio Med.* 44, 1689–1699.
- Lin, C.-C., Chen, S.-J., Huang, K.-L., Hwang, W.-I., Chang-Chien, G.-P., Lin, W.-Y., 2005. Characteristics of metals in nano/ultrafine/fine/coarse particles collected beside a heavily trafficked road. *Environ. Sci. Technol.* 39, 8113–8122.
- Loxham, M., Cooper, M.J., Gerlofs-Nijland, M.E., Cassee, F.R., Davies, D.E., Palmer, M.R., Teagle, D.A., 2013. Physicochemical characterization of airborne particulate matter at a mainline underground railway station. *Environ. Sci. Technol.* 47, 3614–3622.
- Maier, N., Nickel, K.G., Engel, C., Mattern, A., 2010. Mechanisms and orientation dependence of the corrosion of single crystal cordierite by model diesel particulate ashes. *J. Eur. Ceram. Soc.* 30, 1629–1640.
- Marcazzan, G.M., Vaccaro, S., Valli, G., Vecchi, R., 2001. Characterisation of PM10 and PM2.5 particulate matter in the ambient air of Milan (Italy). *Atmos. Environ.* 35, 4639–4650.
- Masiol, M., Harrison, R.M., 2014. Aircraft engine exhaust emissions and other airport-related contributions to ambient air pollution: a review. *Atmos. Environ.* 95, 409–455.
- Minguillón, M.C., Arhami, M., Schauer, J.J., Sioutas, C., 2008. Seasonal and spatial variations of sources of fine and quasi-ultrafine particulate matter in neighborhoods near the Los Angeles–Long Beach harbor. *Atmos. Environ.* 42, 7317–7328.
- Misra, C., Singh, M., Shen, S., Sioutas, C., Hall, P.M., 2002. Development and evaluation of a personal cascade impactor sampler (PCIS). *J. Aerosol Sci.* 33, 1027–1047.
- Nel, A., Xia, T., Mädler, L., Li, N., 2006. Toxic potential of materials at the nanolevel. *Science* 311, 622–627.
- Nel, A.E., Mädler, L., Velegol, D., Xia, T., Hoek, E.M., et al., 2009. Understanding biophysicochemical interactions at the nano-bio interface. *Nat. Mater.* 8, 543.
- Øvrevik, J., Refsnes, M., Låg, M., Holme, J., Schwarze, P., 2015. Activation of proinflammatory responses in cells of the airway mucosa by particulate matter: oxidant- and non-oxidant-mediated triggering mechanisms. *Biomol. Ther.* 5, 1399.
- Pant, P., Harrison, R.M., 2013. Estimation of the contribution of road traffic emissions to particulate matter concentrations from field measurements: a review. *Atmos. Environ.* 77, 78–97.
- Reuter, S., Gupta, S.C., Chaturvedi, M.M., Aggarwal, B.B., 2010. Oxidative stress, inflammation, and cancer: how are they linked? *Free Radic. Bio Med.* 49, 1603–1616.
- Rincon, M., Irvin, C.G., 2012. Role of IL-6 in asthma and other inflammatory pulmonary diseases. *Int. J. Biol. Sci.* 8, 1281.
- Schwarze, P., Øvrevik, J., Låg, M., Refsnes, M., Nafstad, P., Hetland, R., Dybing, E., 2006. Particulate matter properties and health effects: consistency of epidemiological and toxicological studies. *Hum. Exp. Toxicol.* 25, 559–579.
- Shields, L.G., Suess, D.T., Prather, K.A., 2007. Determination of single particle mass spectral signatures from heavy-duty diesel vehicle emissions for PM2.5 source apportionment. *Atmos. Environ.* 41, 3841–3852.
- Shirmohammadi, F., Lovett, C., Sowlat, M., Mousavi, A., Verma, V., Shafer, M., Schauer, J., Sioutas, C., 2017a. Chemical composition and redox activity of PM0.25 near Los Angeles International Airport and comparisons to an urban traffic site. *Sci. Total Environ.* 610, 1336.
- Shirmohammadi, F., Sowlat, M.H., Hasheminassab, S., Saffari, A., Ban-Weiss, G., Sioutas, C., 2017b. Emission rates of particle number, mass and black carbon by the Los Angeles International Airport (LAX) and its impact on air quality in Los Angeles. *Atmos. Environ.* 151, 82–93.
- Sowlat, M.H., Hasheminassab, S., Sioutas, C., 2016. Source apportionment of ambient particle number concentrations in central Los Angeles using positive matrix factorization (PMF). *Atmos. Chem. Phys.* 16, 4849–4866. <https://doi.org/10.5194/acp-16-4849-2016>.
- Touri, L., Marchetti, H., Sari-Minodier, I., Molinari, N., Chanez, P., 2013. The airport atmospheric environment: respiratory health at work. *Eur. Respir. Rev.* 22, 124–130.
- Valberg, P.A., 2004. Is PM more toxic than the sum of its parts? Risk-assessment toxicity factors vs. PM-mortality “effect functions”. *Inhal. Toxicol.* 16, 19–29.
- Wang, Y.-F., Huang, K.-L., Li, C.-T., Mi, H.-H., Luo, J.-H., Tsai, P.-J., 2003. Emissions of fuel metals content from a diesel vehicle engine. *Atmos. Environ.* 37, 4637–4643.
- Xiang, P., He, R.-W., Han, Y.-H., Sun, H.-J., Cui, X.-Y., Ma, L.Q., 2016. Mechanisms of housedust-induced toxicity in primary human corneal epithelial cells: oxidative stress, proinflammatory response and mitochondrial dysfunction. *Environ. Int.* 89, 30–37.